Weak Radiative Decays of K Mesons*†

M. Moshe‡ and P. Singer
Department of Physics, Technion-Israel Institute of Technology, Haifa, Israel
(Received 11 February 1972)

The possibility of a unified description for several weak radiative decays of K mesons is being investigated. In particular, those processes are considered in which the decay mechanism can be related to the strong (or electromagnetic) PVV vertex, namely $K^+ \to e^+\nu\gamma$, $K_2^0 \to \pi^+\pi^-\gamma$, and $K^+ \to \pi^+\gamma\gamma$, in addition to the process $K_2^0 \to \gamma\gamma$, which was treated before. Vector gauge fields with current mixing and octet breaking in the PVV vertex are used, as indicated from a phenomenological Lagrangian model fitting the data on strong and radiative meson decays. For the weak nonleptonic interaction we have considered two alternatives, the current-current "simplest" Hamiltonian suggested recently in connection with $K_2^0 \to \gamma\gamma$ decay, as well as the current-current octet Hamiltonian in the form introduced by Sakurai, both satisfying the $\Delta S = 1$, $\Delta I = \frac{1}{2}$ rule. The experimental upper limit on $K^+ \to e^+\nu\gamma$ imposes limits on a free parameter of the theory related to the SU(3) symmetry breaking in the PVV vertex. Within these limits we calculate the width for $K_2^0 \to \pi^+\pi^-\gamma$, which differs considerably from the SU(3)-symmetric value and is predicted to be close to the present experimental upper limit. In the calculation of $K^+ \to \pi^+\gamma\gamma$ we consider a new class of diagrams, which appear because of the use of vector gauge fields in the Lagrangian. These diagrams involving four-leg vertices are shown to give the dominant contribution to the decay. The calculated rate and spectrum differ from those of previous calculations.

I. INTRODUCTION

In this work we investigate the possibility of obtaining a unified satisfactory theoretical description for a certain class of K-meson radiative decays. To this end we make use of information obtained during recent years from electromagnetic and strong mesonic transitions, which points towards fairly large effects of SU(3) symmetry breaking. In particular, we consider the transitions $K^+ \to e^+\nu\gamma$, $K_2^0 \to \gamma\gamma$,[1] $K_2^0 \to \pi^+\pi^-\gamma$, $K^+ \to \pi^+\gamma\gamma$, and the vector part of K_{e4}, the amplitudes of which have contributions from the pseudoscalar-vector-vector vertex. Recently Brown, Munczek, and Singer[2] used a phenomenological Lagrangian with gauge fields, current mixing and octet breaking in the PVV vertex to fit the observed electromagnetic and strong meson decays (see the Appendix for a short description of the model). The model then predicts large SU(3)-symmetry breaking effects for amplitudes involving strange mesons.[2-5] We expect therefore to find sizable effects of SU(3) symmetry breaking in the decays investigated here, and experimentally there are already some indications of large SU(3) symmetry breaking in electromagnetic processes involving strange mesons.[6,7] A comparison of our model with the experimental data could also provide either further support or possible rejection for the type of SU(3)-symmetry-breaking model suggested in Ref. 2.

In this investigation we choose as the framework for treating the nonleptonic weak processes a current-current CP-conserving Hamiltonian, with the currents dominated respectively by vector and pseudoscalar and pseudovector particles, as suggested by Sakurai.[8] For the transformation properties we consider two possibilities: (1) the original form in which the Hamiltonian behaves like a λ_6 vector of an SU(3) octet[8,9]; (2) as this Hamiltonian leads to difficulties in explaining the rate of $K_2^0 \to \gamma\gamma$,[1,10] as well as in a calculation of K_1^0-K_2^0 mass difference,[11] we consider alternatively the "simplest" $\Delta S = 1$ Hamiltonian (i.e., with a minimum of neutral currents) preserving the $\Delta I = \frac{1}{2}$ rule. The two forms for H_{weak} mentioned above are

$$H^{W}_{(\Delta I=1/2,\ \Delta S=1)} = \frac{2}{\sqrt{2}} G_{\text{NL}} d_{6ab} J_\mu^a(x) J_\mu^b(x) \tag{1}$$

and

$$\bar{H}^{W}_{(\Delta I=1/2,\ \Delta S=1)} = \frac{2}{\sqrt{2}} G_{\text{NL}} \left[J_\mu^1(x) J_\mu^4(x) + J_\mu^2(x) J_\mu^5(x) - J_\mu^3(x) J_\mu^6(x) \right], \tag{2}$$

where

$$J_\mu^a = j_\mu^{Va} + j_\mu^{Aa} \tag{3}$$

and $a, b = 1, \ldots, 8$ are SU(3) indices. The dominance of the currents[8] by the appropriate particles is implemented as follows:

$$j_\mu^{Va} = \frac{m_V^2}{f_V} V_\mu^a, \tag{4a}$$

$$j_\mu^{A_a} = \frac{m_A^2}{f_A} A_\mu^a - C_a \partial_\mu \Phi^a , \tag{4b}$$

with C_π the pion decay constant and f_A, f_V the current-field couplings.

The Hamiltonian (1) was shown to reproduce in the pole approximation[8] the current-algebra results for $K \to 2\pi$,[9] and for baryon nonleptonic parity-violating transitions.[12] Using for G_{NL} a value close to the Fermi constant, i.e.,

$$G_{\mathrm{NL}} = 1.1 \times 10^{-5}/m_p^2 , \tag{5}$$

the correct value for $K_1^0 \to 2\pi$ transition is reproduced, while for the baryon decays a value 25% higher is required.[13]

The Hamiltonian (2) can be obtained from (1) by dropping the $J^6 J^8$ term. Alternatively, starting with a nonleptonic Hamiltonian of current-current type built from charged currents one can ask what would be the minimal addition necessary to accommodate the $\Delta I = \frac{1}{2}$ rule, and it appears that suitable addition of a $J^3 J^6$ term is sufficient. In this way one arrives at the Hamiltonian of Eq. (2), which transforms as members of an octet and a $\underline{27}$ representation of SU(3).

The good results obtained[8] by Sakurai from (1) are still valid when (2) is used as the $J^6 J^8$ term does not contribute to the K and hyperon decays discussed. Albright and Oakes[14] analyzed various experimental data and concluded that a $J^6 J^8$ term is not required by the present data. Moreover, as Hamiltonian (2) was shown[1] to be able to account also for $K_2^0 \to \gamma\gamma$, where (1) fails, there seems to be preference for (2) as compared to the pure octet form (1) originally suggested.

The plan of this paper is as follows: In Sec. II we consider the decay $K^+ \to e^+ \nu\gamma$ and deduce information on the SU(3)-symmetry-breaking parameters ϵ_2. In Sec. III we calculate the decay rate for $K_2^0 \to \pi^+\pi^-\gamma$ under the possible various assumptions for PVV vertices and the nonleptonic weak Hamiltonian. The predicted rate consistent with the framework previously used for $K_2^0 \to \gamma\gamma$ is singled out. In Sec. IV we calculate various contributions to the decay $K^+ \to \pi^+\gamma\gamma$ and show that most of them are insignificant as compared to the contribution of the diagrams with four-leg vertices which appear in our specific Lagrangian. The rate and the pion energy spectrum are then calculated for the latter contributions. The paper concludes with a short discussion in Sec. V.

II. THE DECAY $K^+ \to e^+ \nu\gamma$

The amplitude for this process[15] has an inner-bremsstrahlung contribution as well as a direct one, which can be divided into vector and axial-vector parts. The vector part contain $K^{*+}V^0K^+$ vertex in the vector-dominance picture, and is supposed to proceed $K^+ \to K^{*+}V^0 \to e^+\nu\gamma$, where for V^0 we take the suitable combination of ρ^0, ω^0, ϕ^0. The coupling $g_{K^{*+}V^0K^+}$ can entail large SU(3) symmetry breaking, and this has not yet been determined from electromagnetic and strong processes, which makes this process particularly interesting for our purpose. In this section we deal with the direct vector contribution, which is the only one affected by our model. For the inner-bremstrahlung and direct axial-vector part, we refer the reader to the detailed paper of Carron and Schult.[15]

The amplitude of the vector part of the direct process, $M_{V,D}$, is calculated by using the Lagrangians of Eqs. (A4) and (A8) and the weak Hamiltonian for semileptonic processes:

$$H_{I,V}(\Delta S = 1) = \frac{G_F \sin\theta_C}{\sqrt{2}} (J^h_{V,\alpha} j^{l}_{\alpha} + \mathrm{H.c.}) , \tag{6}$$

where G_F is the Fermi constant, and θ_C is the Cabibbo angle. One obtains

$$M_{V,D}(K^+(P) \to e^+(p) + \nu(q) + \gamma(k)) = -\tfrac{2}{3}\epsilon^{\alpha\beta\mu\nu} \frac{eh}{g} \left(\frac{1 - \frac{1}{2}\epsilon_1 + \frac{3}{4}\epsilon_2}{\sqrt{K_{K^*}}} \right) \frac{G_F \sin\theta_C}{\sqrt{2}} \times \frac{m_{K^*}^2}{f_{K^*}} \frac{k_\alpha \epsilon_\beta (p+q)_\mu \bar{u}(q) \gamma_\nu (1-\gamma_5) v(p)}{(p+q)^2 - m_{K^*}^2} . \tag{7}$$

(Throughout this work, we use units for which $\hbar = c = 1$.) For easy reference we denote

$$V_K = -\frac{2}{3} \frac{h}{g} \left(\frac{1 - \frac{1}{2}\epsilon_1 + \frac{3}{4}\epsilon_2}{\sqrt{K_{K^*}}} \right) \frac{m_{K^*}^2}{f_{K^*}} \frac{1}{(p+q)^2 - m_{K^*}^2} . \tag{8}$$

It is worth remarking here that the vector-dominance assumption (through ρ^0) in the parallel process $\pi \to e\nu\gamma$, gives the same result as calculated from conservation of the vector current (CVC).[15]

The axial-vector part has been studied by several authors, and it is generally concluded that the form-factor of the axial-vector part, defined in a similar way to V_K, satisfies the inequality[15]

$$0 < \frac{A_K(0)}{V_K(0)} < 0.5 . \tag{9}$$

The inner-bremsstrahlung part is exactly calculable, and its contribution becomes negligible in a certain region of the Dalitz plot for this decay. Searching for the decay in this region, one can obtain information on the contribution of the direct part of the amplitude. The best place to look[15,16] for positrons originating from $K^+ \to e^+\nu\gamma$ is the in-

tersection of the above region with that free of positrons from other K^+ decays, which amounts to positrons with energies larger than 228 MeV. In a recent experiment, Macek *et al.*[17] obtained an upper limit for $V_K(0)$ from a search for positrons with energies larger than 234 MeV, namely

$$|V_K(0)| < 0.24/m_K . \tag{10}$$

In obtaining this limit, they assumed $(A_K/V_K) > 0$ and V_K to be independent of $(p+q)^2$. Within the 20% uncertainty that can be caused by the $(p+q)^2$ dependence of V_K in our model, we conclude from (10)

$$\left| \frac{2}{3}\frac{h}{g}\frac{1-\frac{1}{2}\epsilon_1+\frac{3}{4}\epsilon_2}{\sqrt{K_{K^*}}}\frac{1}{f_{K^*}}m_K \right| < 0.24 , \tag{11}$$

which, by using the numerical values in (A9) as well as

$$\left(\frac{m_{K^*}}{f_{K^*}}\right)^2 = \left(\frac{m_\rho}{f_\rho}\right)^2 = \left(\frac{m}{g}\right)^2 ,$$
$$K_{K^*} = \frac{m^2}{m_{K^*}{}^2} , \tag{12}$$

then leads to

$$\left| \frac{1-\frac{1}{2}\epsilon_1+\frac{3}{4}\epsilon_2}{1+\epsilon_1} \right| < 3.3 . \tag{13}$$

This imposes the following limits on ϵ_2 for solutions A and B of Ref. 2:

$$-8.9 < \epsilon_2 < 7.4 , \tag{14a}$$

$$-10.2 < \epsilon_2 < 9.05 . \tag{14b}$$

Hence the present experimental data on $K \to e\nu\gamma$ do not impose severe limits[18] on the breaking parameter ϵ_2. In the following sections additional constraints on ϵ_2 will be obtained.

III. THE DECAY $K_2^0 \to \pi^+\pi^-\gamma$

As the decay $K_2^0 \to \pi^+\pi^-$ is a CP-violating process, the accompanying inner bremsstrahlung (ib) will constitute only a small part of the $K_2^0 \to \pi^+\pi^-\gamma$ transition. For instance, with detecting efficiency $E_\gamma > 20$ MeV, one expects[19]

$$\Gamma^{\text{ib}}_{K_2^0 \to \pi^+\pi^-\gamma} / \Gamma_{K_2^0 \to \text{all}} \simeq 0.8 \times 10^{-5} .$$

This has to be compared with theoretical estimates for the contribution of the direct (d) decay, which give[19]

$$\Gamma^{d}_{K_2^0 \to \pi^+\pi^-\gamma} / \Gamma_{K_2^0 \to \text{all}} \simeq 10^{-4} ,$$

and with the existing experimental upper limit[20] (for $E_\gamma > 20$ MeV):

$$\Gamma^{\text{exp}}_{K_2^0 \to \pi^+\pi^-\gamma} / \Gamma_{K_2^0 \to \text{all}} < 4 \times 10^{-4} . \tag{15}$$

Hence the relative smallness of the bremmstrahlung part makes this decay suitable for a detailed investigation of the structure-dependent (direct) term.

Current-algebra[19] and Veneziano-model[21] type calculations of this process predict a branching ratio of approximately 10^{-4}. Pole-model calculations for this transition have also been performed.[22] Unfortunately, these refer only to some of the possible contributions. Specifically, these works[22] did not include the contribution of the axial-vector mesons to the axial-vector current. Moreover, they did not include vector currents in H^W_{NL} and therefore could not take into account the vector-mesons contribution through these currents (see, e.g., the second diagrams of m_1, m_4 and diagrams m_5, m_6 of Fig. 3 below). There is no *a priori* reason for neglecting all these diagrams, which contribute parity-conserving transitions to the decay under consideration, and indeed their contribution has turned out to be significant.

The lowest transitions in the direct part of the amplitude, considering only CP-conserving transitions, are of magnetic dipole ($M1$) and electric quadrupole ($E2$) types. In this decay, the former is parity conserving and the latter, parity violating. From angular-momentum-barrier considerations the former is expected to dominate by at least an order of magnitude. For instance, a very rough estimate gives[23] for the appropriate transition probabilities

$$W(M, \lambda, k)/W(E, \lambda+1, k) \simeq [(2\lambda+3)^2/(kR)^2][1/(MR)^2] .$$

Using $MR \simeq 1$, and $M \simeq M_K$ for the radiating intermediate state, one obtains $(M1)/(E2) \lesssim 200$ for γ energies $E_\gamma \lesssim E_{\max} = 170$ MeV. Hence we shall retain in the following only the magnetic transition.

We calculate now the $M1$ transition of $K_2^0 \to \pi^+\pi^-\gamma$ by using the Lagrangian of Eq. (A4) and the alternative nonleptonic Hamiltonians of Eqs. (1) and (2). The strong and electromagnetic parts of the amplitude are calculated with vector-meson dominance, while the weak part contains all the poles consistent with the weak Hamiltonian. The axial-vector-current contribution is included using Rockmore's procedure.[24] In Fig. 1 we classify for convenience the contributing diagrams in four classes. The primary strong and electromagnetic vertices are specified in detail, while the blobs are to be calculated by using the specific weak Hamiltonian. When this is done, the detailed resulting structure obtained is presented in Fig. 2, where only the nonvanishing contributions appear. Identical diagrams can appear from different classes when the W_i are calculated in detail, namely when the weak interaction causes a vector-meson $\to$ vector-meson transition in intermediate states. They are obviously not doubly counted. The diagrams appearing in Fig. 2 give contributions to $M1$ as well as to

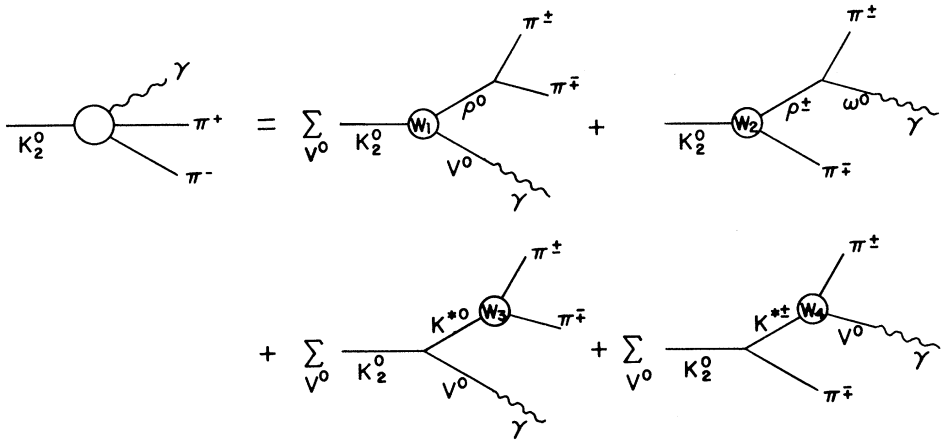

FIG. 1. Contributions to the decay $K_2^0 \to \pi^+\pi^-\gamma$ in the vector dominance model.

higher transitions. We now select the subset of Feynman diagrams contributing to $M1$ transitions, and these are given in Fig. 3. Their explicit calculation gives

$$M^{M1}_{K_2^0\to\pi^+\pi^-\gamma} = \frac{2}{\sqrt{2}} G_{\mathrm{NL}} \left(\frac{m}{g}\right)^2 \frac{eh}{m_{K^0}{}^2} \times \sum_{i=1}^{6} D_i a_i \epsilon^{\alpha\beta\mu\nu} p^+_\alpha p^-_\beta k_\mu \epsilon_\nu , \tag{16}$$

where

$$D_1 = \frac{1}{x-\rho}, \tag{17a}$$

$$D_2 = \frac{1}{y-\rho} + \frac{1}{z-\rho}, \tag{17b}$$

$$D_3 = \frac{1}{x-\kappa}, \tag{17c}$$

$$D_4 = \frac{1}{y-\kappa} + \frac{1}{z-\kappa}, \tag{17d}$$

$$D_5 = \frac{1}{(x-\rho)(x-\kappa)}, \tag{17e}$$

$$D_6 = \frac{1}{(y-\kappa)(y-\rho)} + \frac{1}{(z-\kappa)(z-\rho)} \tag{17f}$$

and

$$x = \left(\frac{p^+ + p^-}{m_{K^0}}\right)^2, \quad y = \left(\frac{p^- + k}{m_{K^0}}\right)^2, \quad z = \left(\frac{p^+ + k}{m_{K^0}}\right)^2, \quad \rho = \left(\frac{m_\rho}{m_{K^0}}\right)^2, \quad \kappa = \left(\frac{m_{K^*}}{m_{K^0}}\right)^2, \quad x+y+z = 1 + \frac{2m_{\pi^+}{}^2}{m_{K^0}{}^2}. \tag{18}$$

The a_i are related to the explicit form of the PVV and PPV vertices and the nonleptonic Hamiltonian. For Sakurai's version [Eq. (1)], they are

$$a_1 = \frac{2}{3}\frac{C_K}{C_\pi}\left(\frac{m_{\pi^0}{}^2}{m_{K^0}{}^2 - m_{\pi^0}{}^2}\right)\left(\frac{1+\epsilon_1}{K_\rho}\right) + \frac{1}{3}\frac{C_\eta C_K}{C_\pi{}^2}\left(\frac{m_\eta{}^2}{m_{K^0}{}^2 - m_\eta{}^2}\right)\left(\frac{1-\epsilon_1+\epsilon_2+\epsilon_3}{K_\rho}\right) - \frac{8}{3}\frac{m_\rho}{m_{K^*}}\left(\frac{1-\frac{1}{2}\epsilon_1+\frac{1}{4}\epsilon_2}{(K_{K^*}K_\rho)^{1/2}}\right)$$
$$= 0.045(1+\epsilon_1) - 1.87(1-\epsilon_1+\epsilon_2+\epsilon_3) - 2.17(1-\tfrac{1}{2}\epsilon_1+\tfrac{1}{4}\epsilon_2), \tag{19a}$$

$$a_2 = \frac{2}{3}\frac{C_K}{C_\pi}\left(\frac{m_{\pi^0}{}^2}{m_{K^0}{}^2 - m_{\pi^0}{}^2} + \frac{1}{2}\frac{m_{K^+}{}^2}{m_{\pi^+}{}^2 - m_{K^+}{}^2}\right)\left(\frac{1+\epsilon_1}{K_\rho}\right) = -0.27(1+\epsilon_1), \tag{19b}$$

$$a_3 = \frac{4}{3}\frac{C_K}{C_\pi}\left(\frac{m_{K^+}{}^2}{m_{K^+}{}^2 - m_{\pi^+}{}^2}\right)\left(\frac{1-\frac{1}{2}\epsilon_1}{(K_\rho K_{K^*})^{1/2}}\right) = 1.49(1-\tfrac{1}{2}\epsilon_1), \tag{19c}$$

$$a_4 = \frac{1}{3}\frac{C_K}{C_\pi}\left(\frac{m_{K^+}{}^2}{m_{\pi^+}{}^2 - m_{K^+}{}^2}\right)\left(\frac{1-\frac{1}{2}\epsilon_1+\frac{3}{4}\epsilon_2}{(K_\rho K_{K^*})^{1/2}}\right) - \frac{4}{3}\left(\frac{1+\epsilon_1-\frac{1}{2}\epsilon_2}{(K_\rho K_{K^*})^{1/2}}\right)$$
$$= -0.37(1-\tfrac{1}{2}\epsilon_1+\tfrac{3}{4}\epsilon_2) - 1.26(1+\epsilon_1-\tfrac{1}{2}\epsilon_2), \tag{19d}$$

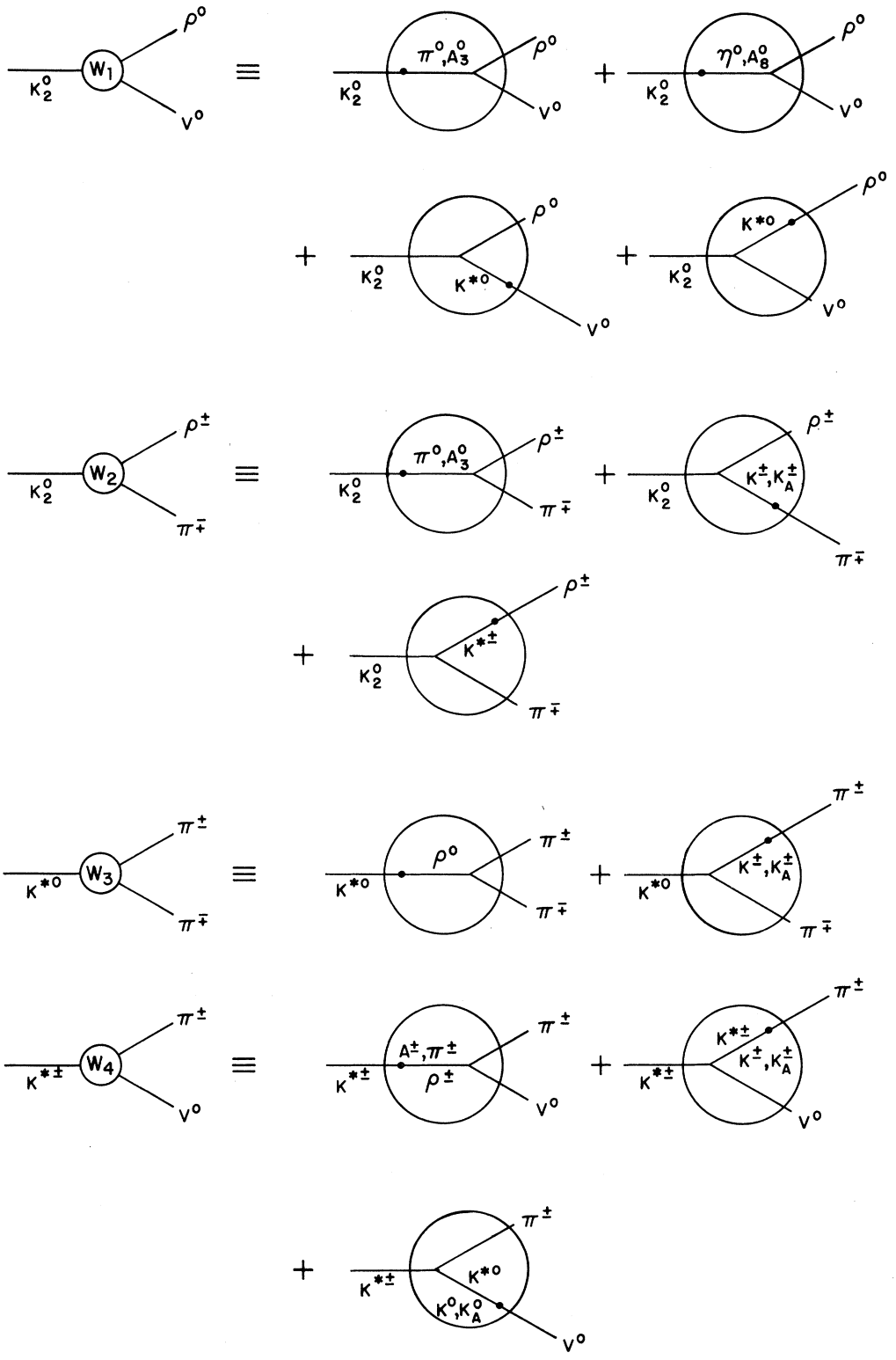

FIG. 2. Nonvanishing contributions to the "structures" W_i of Fig. 1, calculated by the use of Eq. (1); when Eq. (2) is used instead of Eq. (1), the contributions containing a 6-8 weak transition disappear.

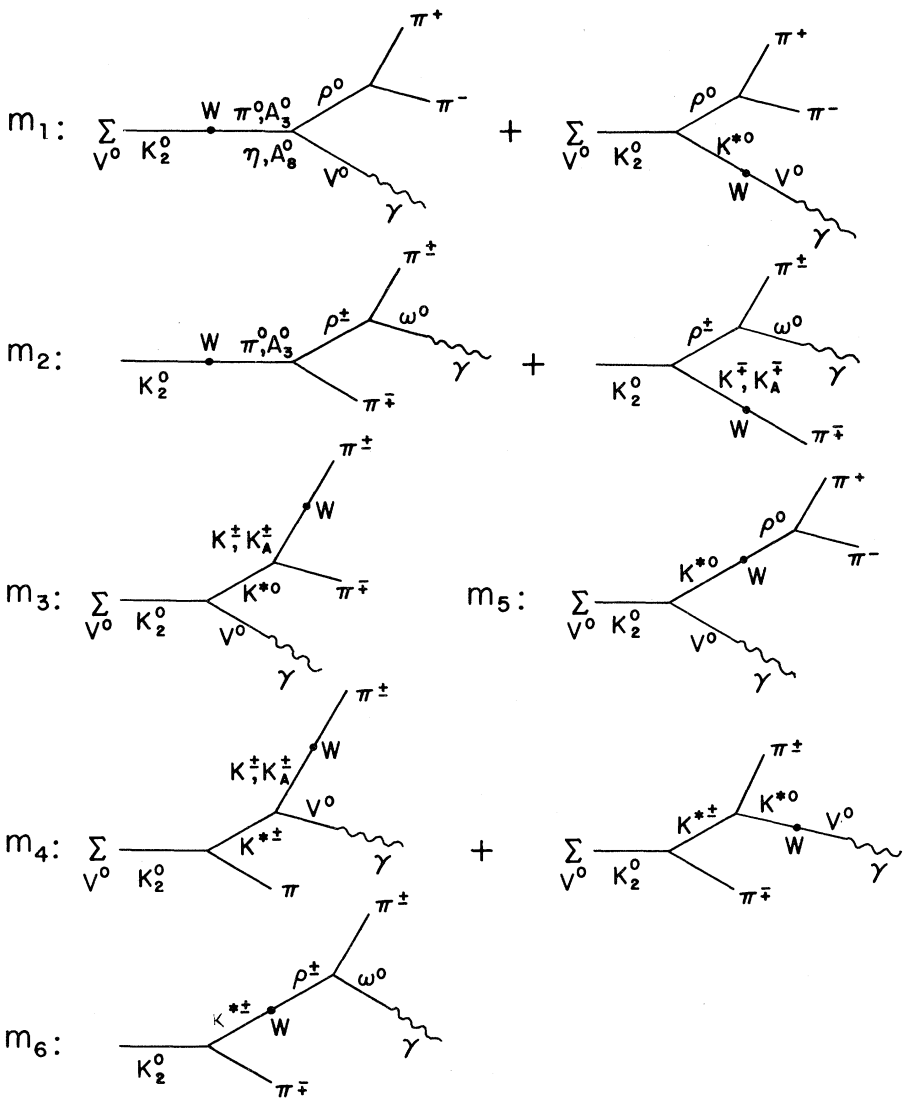

FIG. 3. Feynman diagrams contributing to the $M1$ transition of $K_2^0 \to \pi^+\pi^-\gamma$. The diagrams exhibited arise from the use of Eq. (1) for the weak Hamiltonian. When Eq. (2) is used for it, the diagrams containing 6-8 weak transitions disappear.

$$a_5 = \frac{8}{3}\left(\frac{m_{K^*}m_\rho}{m_{K^0}{}^2}\right)\left(\frac{1-\frac{1}{2}\epsilon_1}{(K_{K^*}K_\rho)^{1/2}}\right) = 6.95(1-\tfrac{1}{2}\epsilon_1)\,, \tag{19e}$$

$$a_6 = \frac{2}{3}\left(\frac{m_{K^*}m_\rho}{m_{K^0}{}^2}\right)\left(\frac{1+\epsilon_1}{K_\rho}\right) = 1.5(1-\epsilon_1)\,. \tag{19f}$$

When the "simplest" Hamiltonian [Eq. (2)] is used, a_2, a_3, a_5, and a_6 remain unchanged and for a_1 and a_4 one has

$$\bar{a}_1 = \frac{2}{3}\frac{C_K}{C_\pi}\left(\frac{m_{\pi^0}{}^2}{m_{K^0}{}^2 - m_{\pi^0}{}^2}\right)\left(\frac{1+\epsilon_1}{K_\rho}\right) - 2\frac{m_\rho}{m_{K^*}}\left(\frac{1-\frac{1}{2}\epsilon_1+\frac{1}{4}\epsilon_2}{(K_{K^*}K_\rho)^{1/2}}\right)$$
$$= 0.045(1+\epsilon_1) - 1.63(1-\tfrac{1}{2}\epsilon_1+\tfrac{1}{4}\epsilon_2)\,, \tag{20a}$$

$$\bar{a}_4 = \frac{1}{3}\frac{C_K}{C_\pi}\left(\frac{m_{K^+}{}^2}{m_{\pi^+}{}^2 - m_{K^+}{}^2}\right)\left(\frac{1-\frac{1}{2}\epsilon_1+\frac{3}{4}\epsilon_2}{(K_\rho K_{K^*})^{1/2}}\right) - \frac{1+\epsilon_1-\frac{1}{2}\epsilon_2}{(K_\rho K_{K^*})^{1/2}}$$
$$= -0.37(1-\tfrac{1}{2}\epsilon_1+\tfrac{3}{4}\epsilon_2) - 0.95(1+\epsilon_1-\tfrac{1}{2}\epsilon_2)\,. \tag{20b}$$

numerical values in (19) and (20) are obtained by using Eq. (12), with m and g given in the Appendix, as well as[25]

$$C_\eta = 1.13 C_\pi\,, \quad C_K = 1.08 C_\pi\,. \tag{21}$$

For C_π and the various masses entering in (18), (19) we use the tabulated values.[26]

Calculating the contribution to the decay width from the $M1$ transition we find the following: With SU(3)-symmetric PVV vertices ($\epsilon_i \to 0$), one obtains with Sakurai's Hamiltonian

$$\Gamma^{\mathrm{SU(3)}}_{K_2^0 \to \pi^+\pi^-\gamma}/\Gamma_{K^0 \to \mathrm{all}} = 39 \times 10^{-4}\,, \tag{22}$$

and with the "simplest" Hamiltonian,

$$\overline{\Gamma}^{\mathrm{SU(3)}}_{K_2^0 \to \pi^+\pi^-\gamma}/\Gamma_{K_2^0 \to \mathrm{all}} = 18 \times 10^{-4}\,. \tag{23}$$

Both results are well above the experimental upper limit [Eq. (15)].

When SU(3) symmetry breaking is taken into account, the result depends on ϵ_1, $(\epsilon_2 + \epsilon_3)$, and ϵ_2. Solutions (A) and (B) of the Appendix give possible values for ϵ_1 and $(\epsilon_2 + \epsilon_3)$ obtained from fitting the electromagnetic decays. The appropriate values of ϵ_2 were shown in Sec. II to be limited [see Eq. (14)] by the experimental upper limit on $K^+ \to e^+\nu\gamma$.

With Solution (A) we find that both Hamiltonians give ranges above the experimental upper limit, namely

$$17 \times 10^{-4} < \Gamma^{A}_{K_2^0 \to \pi^+\pi^-\gamma}/\Gamma_{K_2^0 \to \mathrm{all}} < 24 \times 10^{-4} \tag{24}$$

and

$$4 \times 10^{-4} < \overline{\Gamma}^{A}_{K_2^0 \to \pi^+\pi^-\gamma}/\Gamma_{K_2^0 \to \mathrm{all}} < 9 \times 10^{-4}\,. \tag{25}$$

This is evidence that solution (A) of the Appendix is ruled out by this decay. Nevertheless, if the process is found to occur with a strength close to the present experimental upper limit, this will still be consistent with the lower limit (i.e., $\epsilon_2 = -8.9$) calculated using the "simplest" Hamiltonian and solution (A).

Solution (B) gives solutions consistent with experiment for both Hamiltonians, as follows:

$$0.4 \times 10^{-4} < \Gamma^{B}_{K_2^0 \to \pi^+\pi^-\gamma}/\Gamma_{K_2^0 \to \mathrm{all}} < 1.6 \times 10^{-4}\,, \tag{26}$$

and

$$2.6 \times 10^{-4} < \overline{\Gamma}^{B}_{K_2^0 \to \pi^+\pi^-\gamma}/\Gamma_{K_2^0 \to \mathrm{all}} < 7 \times 10^{-4}\,. \tag{27}$$

The above results are given graphically in Figs. 4 and 5.

Using the information obtained from $K_2^0 \to \gamma\gamma$,[1] which disqualifies Sakurai's form (1), we can now predict the $M1$ transition $K_2^0 \to \pi^+\pi^-\gamma$ to occur at a rate

$$2.6 \times 10^{-4} < \Gamma^{M1}_{K_2^0 \to \pi^+\pi^-\gamma}/\Gamma_{K_2^0 \to \mathrm{all}} < 4 \times 10^{-4}\,. \tag{28}$$

The ϵ_2 is then further limited to the range

$$-10.2 < \epsilon_2 < -4.5\,. \tag{29}$$

These values of ϵ_2 then imply a $K^{*+} \to K^+\gamma$ transition[2] increased by 1.4–11 over the SU(3) value.

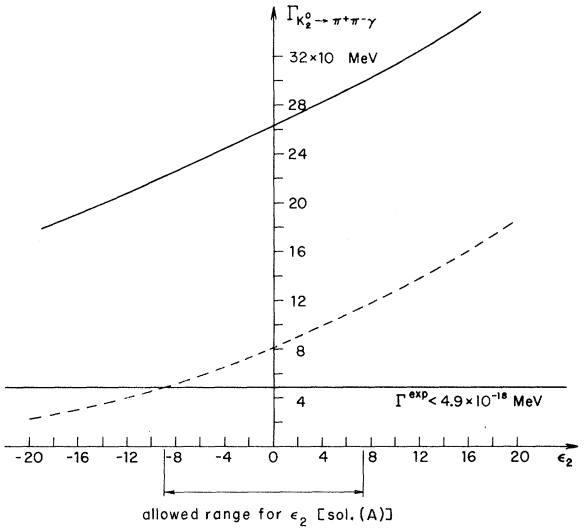

FIG. 4. The decay width of $K_2^0 \to \pi^+\pi^-\gamma$, calculated with parameters of solution (A) [Eq. (A10)], as a function of the SU(3)-symmetry-breaking parameter ϵ_2. The allowed range for ϵ_2 is determined from the upper limit of $K^+ \to e^+\nu\gamma$. The calculation is performed with two alternatives for the weak Hamiltonian: Eq. (1) – unbroken line; Eq. (2) – broken line.

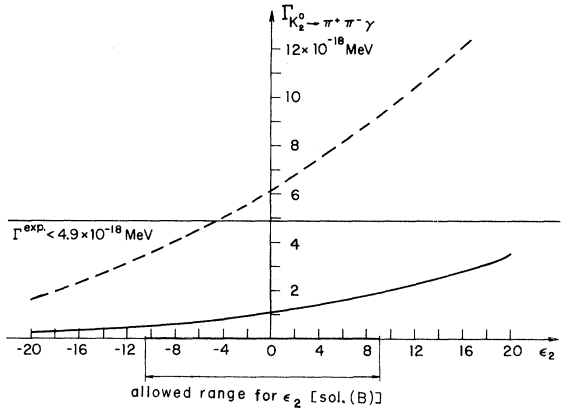

FIG. 5. The decay width of $K_2^0 \to \pi^+\pi^-\gamma$, calculated with parameters of solution (B) [Eq. (A11)], as a function of the SU(3)-symmetry-breaking parameter ϵ_2. The allowed range for ϵ_2 is determined from the upper limit of $K^+ \to e^+\nu\gamma$. The calculation is performed with two alternatives for the weak Hamiltonian: Eq. (1) – unbroken line; Eq. (2) – broken line.

IV. THE DECAY $K^+ \to \pi^+ \gamma\gamma$

A. General Considerations

We now employ the Lagrangian of Eq. (A4), together with the weak Hamiltonian of Eq. (1) or Eq. (2) in order to calculate the partial width of $K^+ \to \pi^+ \gamma\gamma$. The latest[27] experimental upper limit for this process gives[28] for the branching ratio

$$R_B = \frac{\Gamma_{K^+ \to \pi^+ \gamma\gamma}}{\Gamma_{K^+ \to \text{all}}} < 4 \times 10^{-5} \tag{30a}$$

or

$$\Gamma_{K^+ \to \pi^+ \gamma\gamma} < 2.13 \times 10^{-18}\ \text{MeV}. \tag{30b}$$

In Fig. 6 we exhibit the seven classes of diagrams contributing in our model. Previous calculations of this process usually dealt with the contribution of a particular diagram. The pion-pole model suggested by Lapidus[29] gives a very small contribution, when the 2γ's are away from the pion mass shell. This model is, however, of special interest as it relates the $K^+ \to \pi^+ \gamma\gamma$ decay to the $K^+ \to \pi^+ \pi^0$ transition, and with a $\Delta I = \frac{1}{2}$ weak Hamiltonian the radiative process may be directly related[8,30] to the π^+-π^0 mass difference. With a linear extrapolation in $(p^{\pi^0})^2$ off the mass shell, Fujii obtained[31] a fairly high rate for the process, i.e., $R_B(\pi^0) = 2.7 \times 10^{-5}$ (considering the total energy of the two photons larger than $1.5 m_\pi$). Calculations with an η^0 pole lead to a small[32] contribution, $R_B(\eta) = 1.4 \times 10^{-6}$ (for $0 < T_{\pi^+} < 70$ MeV). Calculations with the vector-dominance-model have shown that when one takes an SU(3)-symmetric PVV vertex, such contributions[31] are three orders of magnitude below the experimental upper limit. Recently a calculation was done by Intemann,[33] assuming axial-vector-meson dominance.

By the use of the weak Hamiltonian [Eq. (1) or (2)] the detailed resulting structure of the weak blobs is obtained for the various classes of Fig. 6. We present our results by dividing the contributing Feynman diagrams into several groups. As it turns out from the detailed calculation, the first five groups give relatively small contributions and are only briefly described in Sec. IV B.[34] The last group which is related to four-leg vertices and is likely to be the dominant contributor is described in Sec. IV C.

B. Various Small Contributions to $\Gamma_{K^+ \to \pi^+ \gamma\gamma}$

In group I of the diagrams obtained from Fig. 6 we classify the diagrams with two PVV vertices. They are presented in Fig. 7. Some of these contributions to the width were previously estimated by Fujii.[31] Similarly to what was explained in Sec.

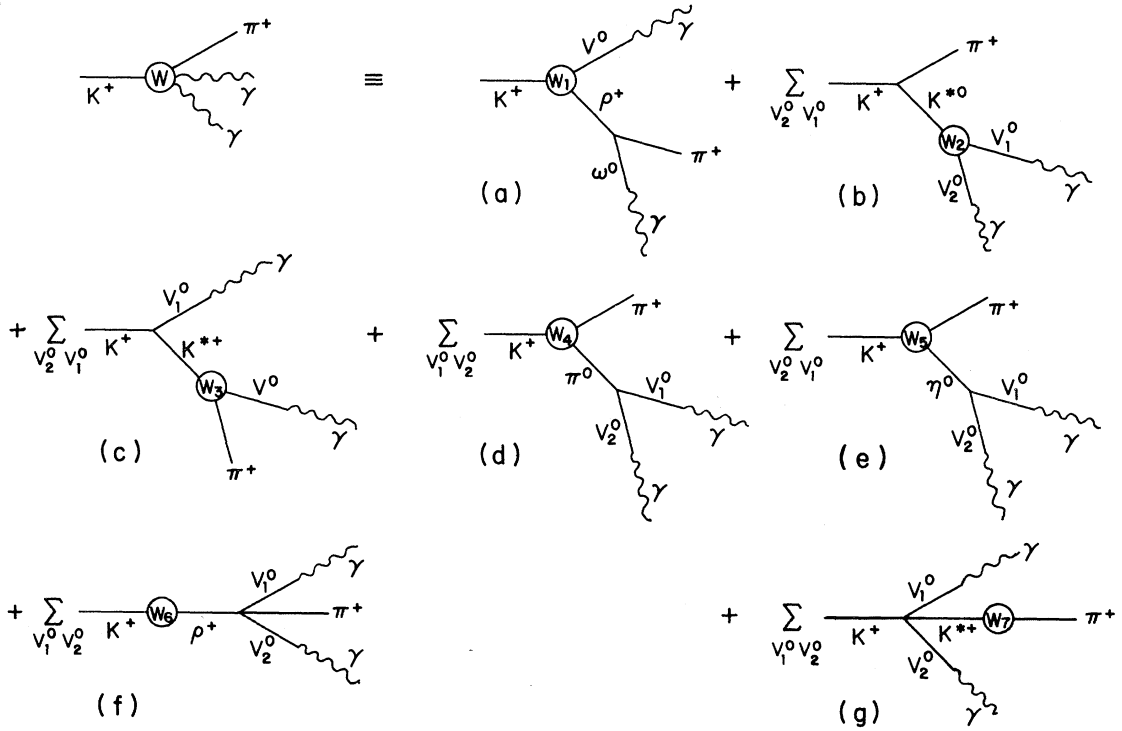

FIG. 6. The seven classes of diagrams contributing to $K^+ \to \pi^+ \gamma\gamma$ in the model of this paper.

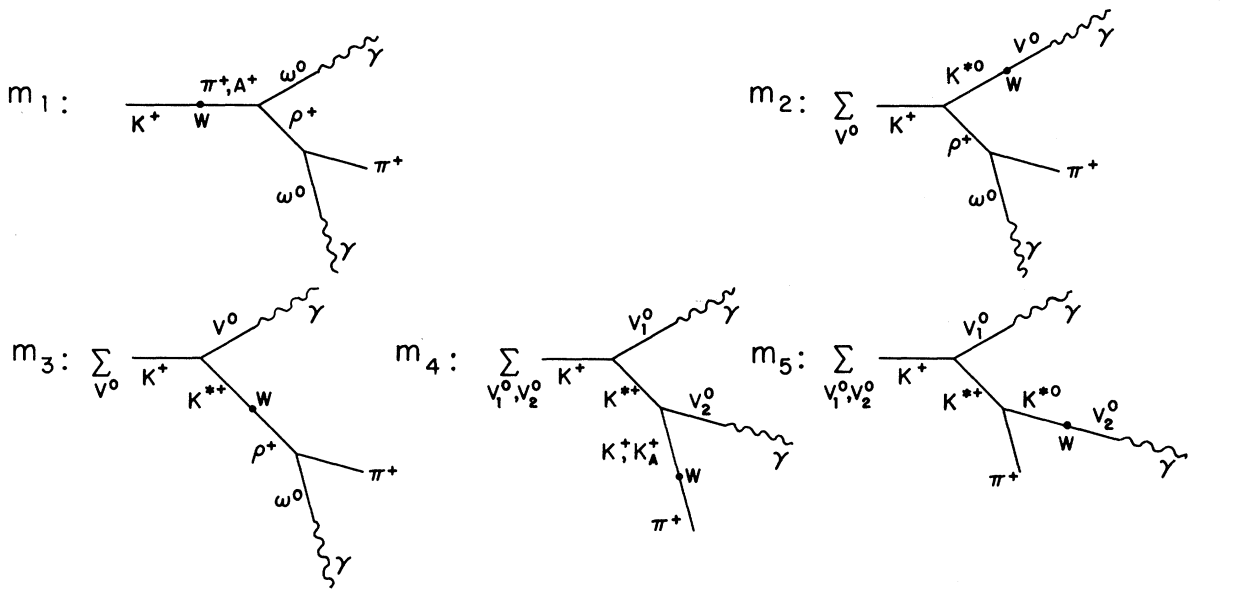

FIG. 7. Group of Feynman diagrams with two PVV vertices, obtained from the contributions exhibited in Fig. 6.

III, we include the axial-vector current contribution with Rockmore's procedure,[24] and the numerical values are obtained by using Eqs. (12) and (21) with m and g given in the Appendix.

Firstly, with Sakurai's weak Hamiltonian we obtain in the SU(3) case ($\epsilon_i \to 0$)

$$\Gamma_I^{SU(3)} = 0.15 \times 10^{-20}\ \text{MeV}, \tag{31}$$

which is three orders of magnitude below the experimental limit. Including SU(3) symmetry breaking, we get for the two possible solutions [Eqs. (A10), (A11) and Eqs. (14a), (14b) for the limits on ϵ_2 as deduced from $K^+ \to e^+\nu\gamma$]

$$0.6 \times 10^{-20} < \Gamma_I^A < 7.1 \times 10^{-20}\ \text{MeV}, \tag{32a}$$

$$10^{-20} < \Gamma_I^B < 6.8 \times 10^{-20}\ \text{MeV}. \tag{32b}$$

Although the SU(3)-symmetry-breaking factors in the PVV vertices appeared in Γ_I at their fourth power, the calculated values given above [with a possible SU(3)-symmetry-breaking effect which multiplies the symmetry value of Eq. (31) by a factor of ≤ 47] are still well below the present experimental upper limit [Eq. (30)].

With the "simplest" nonleptonic Hamiltonian [Eq. (2)] the predictions are again of a small contribution:

$$\overline{\Gamma}_I^{SU(3)} = 0.1 \times 10^{-20}\ \text{MeV}, \tag{33}$$

$$0.1 \times 10^{-20} < \overline{\Gamma}_I^A < 2.5 \times 10^{-20}\ \text{MeV}, \tag{34a}$$

$$0.16 \times 10^{-20} < \overline{\Gamma}_I^B < 2.3 \times 10^{-20}\ \text{MeV}. \tag{34b}$$

In group II we classify diagrams in which one of the photons is emitted from an intermediate vector particle like $K^+ \xrightarrow{W} \rho^+ \to \rho^+\gamma \to \pi^+\gamma\gamma$. Their calculation shows that these diagrams do not contribute more than 10^{-22}–10^{-21} MeV to the partial width.

To group III belong diagrams with one PVV and one PVA vertex when the axial-vector particle is weakly coupled to a vector particle. As an example we mention $K^+ \to \rho^+ K_A^0 \xrightarrow{W} \rho^+ V^0 \to \rho^+\gamma \to \pi^+\gamma\gamma$. This type of diagram cannot be treated with Rockmore's procedure,[10,24] and the knowledge of the strength of the PVA coupling is needed. With reasonable estimates for the $A \to \rho\pi$ width and the g_T/g_L ratio,[35] these diagrams contribute less than 3×10^{-21} MeV.

The fourth group has diagrams with the weak interaction mediating vector to axial-vector transitions, and the γ rays originating from the axial-vector meson. There are two diagrams in this category, namely $K^+ \to \pi^+ K^{*0} \xrightarrow{W} \pi^+ A_3^0(A_8^0) \to \pi^+\gamma\gamma$. As in the previous group (III) the axial-vector intermediate state must be treated separately, and an estimate of the $A\gamma\gamma$ coupling is needed. For this estimate we used the partial conservation of tensor current hypothesis (see, e.g., Maiani and Preparata[36] and Zimmerman and Savoy[37]). These contributions amount to approximately 10^{-20} MeV.

Our fifth group contains the π^0- and η^0-pole diagrams presented in Fig. 8. In this calculation we include also η-π^0 mixing, which is determined so as to give the observed value for the $K^+ \to \pi^+\pi^0$ transition. Since this point is of more general relevance, we give here details of our treatment of η-π mixing.

As the weak Hamiltonians (1) and (2) are unable to account for $K^+ \to \pi^+\pi^0$ (Okubo *et al.*[30]), we should be able to account correctly for this physical pro-

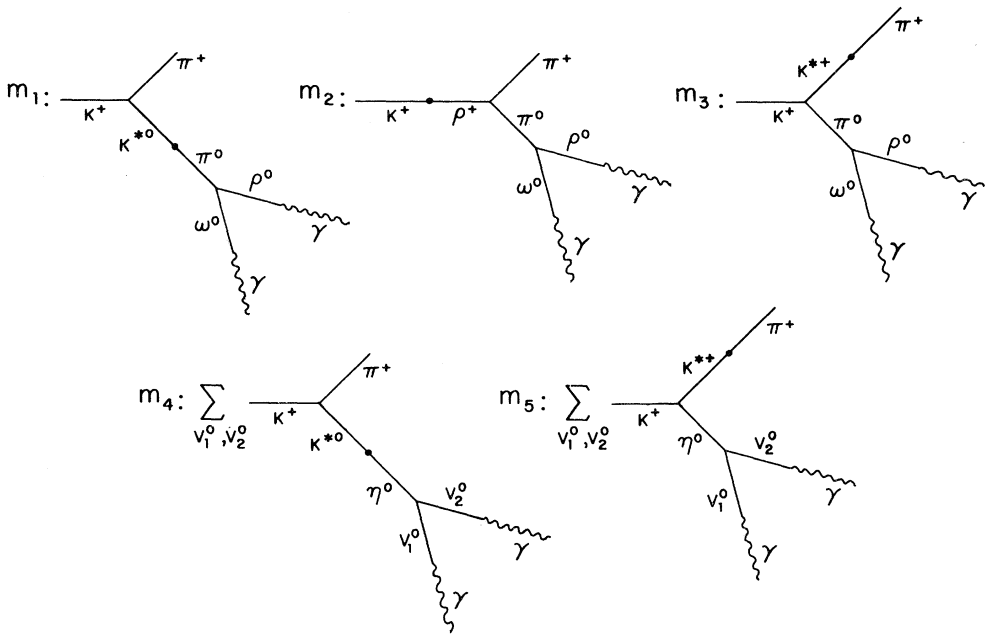

FIG. 8. The group of π^0- and η^0-pole diagrams.

cess before using the $K\pi\pi$ vertex in the pion-pole description of $K \to \pi\gamma\gamma$. This is done here by our using a π^0-η^0 mixing term of the form[38]

$$H = \tilde{\lambda} j_\mu^{A3} j_\mu^{A8} \tag{35}$$

in conjunction with the weak Hamiltonian, and we then determine $\tilde{\lambda}$ by comparing the calculated $K^+ \to \pi^+\pi^0$ width to the experimental value. One obtains, using the weak Hamiltonians of Eqs. (1) and (2),

$$\tilde{\lambda}_{(1)} = -8.35\times10^{-6}\ \text{MeV}^{-2} \text{ or } 7.35\times10^{-6}\ \text{MeV}^{-2}$$
$$\tilde{\lambda}_{(2)} = -11.5\times10^{-6}\ \text{MeV}^{-2} \text{ or } 12.9\times10^{-6}\ \text{MeV}^{-2}. \tag{36}$$

The decay width is calculated after we have excluded a region of 2 MeV around the π^0 mass in the $k_{\gamma_1}+k_{\gamma_1}$ spectrum. The result obtained is $\sim10^{-22}$ MeV for solution (A) and $\sim10^{-21}$ MeV for solution (B), for both values of $\tilde{\lambda}$.

As a last point in this section, we remark that from gauge-invariance considerations, the radiative contributions from π^+ and K^+ lines are found to vanish.[31]

C. Four-Particle-Vertex Diagrams

The last group, which is found in our model to be the dominant contributor to the amplitude, refers to a class of diagrams (four-particle-vertex diagrams) which was not considered before and is related to the use of a phenomenological Lagrangian with vector-gauge particles. The PVV part of the Lagrangian of Eq. (A4) entails also four-particle vertices by virtue of the "self-interaction" term appearing in $V_{\mu\nu}$ [see Eq. (A5)]. These additional four-particle vertices generated by the $V\times V$ term have their strength determined by the three-particle ones, this being a direct result of the Yang-Mills form of the Lagrangian. The diagrams contributing here are (f) and (g) in Fig. 6.

The matrix element for these diagrams is

$$M_{(K^+\to\pi^+\gamma\gamma)} = \frac{4}{3}\frac{G_{\rm NL}}{\sqrt{2}}\left(\frac{e}{g}\right)^2 h\epsilon^{\alpha\beta\mu\nu}\Big\{C_K(1+\epsilon_1)\Big[P_\nu^{K^+}\epsilon_\beta^1\epsilon_\mu^2(k^1-k^2)_\alpha + P_\nu^{K^+}k_\alpha^2 k_\beta^1\Big(\frac{P^K\cdot\epsilon^1}{P^K\cdot k^1}\epsilon_\mu^2 - \frac{P^K\cdot\epsilon^2}{P^K\cdot k^2}\epsilon_\mu^1\Big)\Big]$$
$$- C_\pi(1-\tfrac{1}{2}\epsilon_1+\tfrac{3}{4}\epsilon_2)\Big[P_\nu^{\pi^+}\epsilon_\beta^1\epsilon_\mu^2(k^1-k^2)_\alpha + P_\nu^{\pi^+}k_\alpha^2 k_\beta^1\Big(\frac{P^K\cdot\epsilon^1}{P^K\cdot k^1}\epsilon_\mu^2 - \frac{P^K\cdot\epsilon^2}{P^K\cdot k^2}\epsilon_\mu^1\Big)\Big]\Big\}. \tag{37}$$

This is substituted in the expression for the partial width:

$$\Gamma_{K^+\to\pi^+\gamma\gamma} = \frac{m_K}{64}\frac{1}{(2\pi)^3}\int_0^{(1/2)(1-m_\pi/m_K)^2} 2dt \int_{m_\pi/m_K+t-[2(m_\pi/m_K)t+t^2]^{1/2}}^{m_\pi/m_K+t+[2(m_\pi/m_K)t+t^2]^{1/2}} dx \sum_{\rm pol}|M|^2\,, \tag{38}$$

where $t = T_{\pi^+}/m_K$, T_{π^+} being the pion kinetic energy, and $x = [(P^\pi + k^1)/m_K]^2$.

After we sum over the two-photon polarization states, we get for the partial width (given in MeV)

$$\Gamma_{K^+\to\pi^+\gamma\gamma}=10^{-18}\int_0^{(1/2)(t-m_\pi/m_K)^2}dt\left|2.2[F_1(t)+F_2(t)]+1.9\left(\frac{1-\frac{1}{2}\epsilon_1+\frac{3}{4}\epsilon_2}{1+\epsilon_1}\right)^2\left[\left(\frac{m_\pi}{m_K}\right)^2F_1(t)+F_2(t)+F_3(t)\right]\right.$$
$$\left.-4.1\left(\frac{1-\frac{1}{2}\epsilon_1+\frac{3}{4}\epsilon_2}{1+\epsilon_1}\right)\left[\left(t+\frac{m_\pi}{m_K}\right)F_1(t)+F_2(t)+F_3(t)\right]\right|, \tag{39}$$

where $\mu=m_\pi/m_K$,

$$F_1(t)=-2(2\mu t+t^2)^{1/2}[4t-2(1-\mu)^2], \tag{40a}$$

$$F_2(t)=\tfrac{4}{3}(2\mu t+t^2)^{3/2}-4[(1-\mu)^2-2t]\left\{(1-t-\mu)\ln\left(\frac{1-t-\mu+(2t\mu+t^2)^{1/2}}{1-t-\mu-(2t\mu+t^2)^{1/2}}\right)-2(2t\mu+t^2)^{1/2}\right\}, \tag{40b}$$

$$F_3(t)=8(2t\mu+t^2)^{1/2}[(1-\mu)^2-2t][1-\mu-t]-4[(1-\mu)^2-2t]\ln\left(\frac{1-t-\mu+(2t\mu+t^2)^{1/2}}{1-t-\mu-(2t\mu+t^2)^{1/2}}\right). \tag{40c}$$

In calculating the decay width with (37), it is immaterial which weak Hamiltonian is used, as we have no 6-8 transition here. In the SU(3)-symmetric case, we get

$$\frac{\Gamma^{SU(3)}_{K^+\to\pi^+\gamma\gamma}}{\Gamma_{K^+\to\text{all}}}=0.56\times10^{-6}, \tag{41}$$

which is two orders of magnitude below the experimental limit. When SU(3) symmetry breaking is included, the resulting width is presented in Fig. 9. The difference between solutions (A) and (B) is slight. It also appears that for large negative values of ϵ_2 the predicted width is quite close to the existing experimental upper limit. From our previous considerations on $K_2^0\to\gamma\gamma$[1] and $K_2^0\to\pi^+\pi^-\gamma$ (see Sec. III) we were led to further limits on ϵ_2, namely $-10.2<\epsilon_2<-4.5$. Hence $K^+\to\pi^+\gamma\gamma$ should be expected to occur with a strength 2–5 times lower than the present experimental limit. As we have already remarked, the allowed range for ϵ_2 implies a $K^{*+}\to K^+\gamma$ transition larger by a factor of 1.4–11 than the SU(3) value.

The energy spectrum of the pion is quite different in our model, as opposed to the pion-pole[29,31] or the axial-vector-meson dominance models[33] (which are the previously suggested models predicting branching ratios close to the experimental limit). The comparison of our prediction [given in Eqs. (39) and (40)] with those of the above models is presented in Fig. 10 for five different values of ϵ_2.

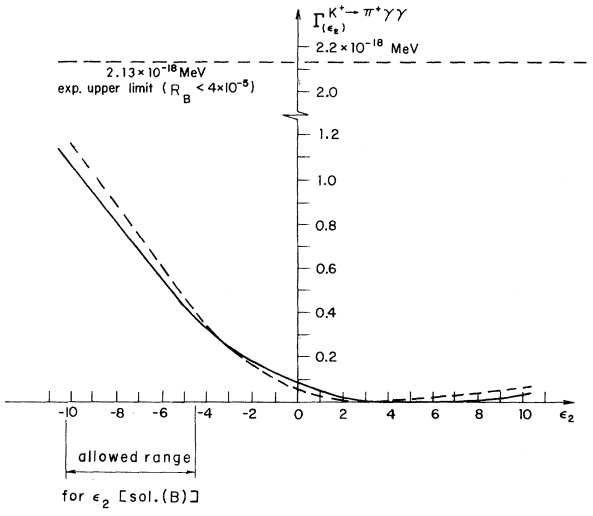

FIG. 9. The partial decay width for $K^+\to\pi^+\gamma\gamma$, as a function of ϵ_2, calculated from diagrams (f) and (g) of Fig. 6 for solution (A) (broken line) and solution (B) (unbroken line). The range for ϵ_2 [solution (B)] is deduced [see Eq. (29)] from considerations on $K^+\to e^+\nu\gamma$, $K_2^0\to\gamma\gamma$, and $K_2^0\to\pi^+\pi^-\gamma$. See discussion in the text following Eq. (25) on the very limited range of values of ϵ_2 [solution (A)] consistent with the above decays.

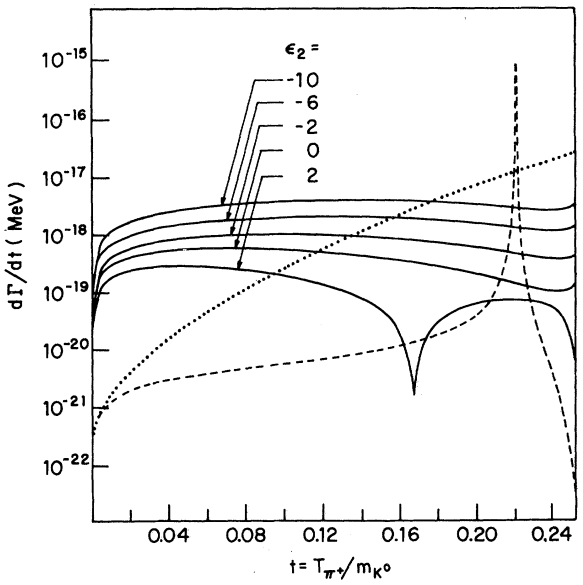

FIG. 10. Comparison of pion kinetic energy spectra obtained with various models for $K^+\to\pi^+\gamma\gamma$. (a) Unbroken line: present calculation with four-particle vertices (for different values of ϵ_2); (b) dotted line: axial-vector dominance model (Ref. 33); (c) dashed line: pion-pole model (Ref. 29).

It is apparent that the striking difference is the near constancy of our spectrum, as compared with that obtained in other models.

V. CONCLUSIONS

We have applied here a phenomenological Lagrangian with vector gauge fields and SU(3)-symmetry-broken PVV and $PVVV$ (related) vertices to calculate various radiative decays of K mesons. The purpose of this investigation is two-fold: As the model[2] applied to electromagnetic decays suggested large effects for strange-particle vertices, it should be possible to check it in radiative K decays; moreover, we are striving to obtain a unified description for all the K-radiative decays obtainable from the model described in the Appendix. In the course of the investigation we also encounter[1] the problem of the suitable weak nonleptonic Hamiltonian for $\Delta S=1$ transitions.

From our previous work[1] on $K_2^0 \to \gamma\gamma$, as well as from the consideration of the decays $K^+ \to e^+\nu\gamma$, $K_2^0 \to \pi^+\pi^-\gamma$, and $K^+ \to \pi^+\gamma\gamma$ in the present article, we find that a suitable description for the considered class of radiative K decays can be offered with the following scheme: (a) The nonleptonic $\Delta S=1$ weak Hamiltonian is given by Eq. (2), i.e., the "simplest" current-current form embodying the $\Delta I=\frac{1}{2}$ rule, and without octet properties[39]; (b) the PVV interaction should be of the broken-type, as evolving from the strong and electromagnetic decays,[2,3] and the preferred solution for the ϵ_i breaking parameters as deduced from the present work is as follows:

$$\epsilon_1=1.2, \quad \epsilon_2+\epsilon_3=-2.5, \quad -10<\epsilon_2<-4.5. \tag{42}$$

The framework containing (a) and (b) is consistent with the following experimental data: (a) the $K_1^0 \to \pi^+\pi^-$ rate; (b) the $K_2^0 \to \gamma\gamma$ rate; (c) the upper limit for $K_2^0 \to \pi^+\pi^-\gamma$; (d) the upper limit for $K^+ \to \pi^+\gamma\gamma$; (e) the upper limit for $K^+ \to e^+\nu\gamma$, as well as the previous results mentioned in Refs. 2 and 3.

It was previously shown[1] that in order to obtain agreement with experiment in the $K_2^0 \to \gamma\gamma$ transition, one is led to include in the formalism SU(3)-symmetry-broken PVV vertices, as well as the form of Eq. (2) for the nonleptonic weak Hamiltonian. In the present paper we have extended the application of the framework concluded in Ref. 1 so as to include the other decays that can be treated by our model. In Sec. II we obtained from the experimental upper limit on $K^+ \to e^+\nu\gamma$ certain bounds on the possible values for the breaking parameter ϵ_2. In Sec. III, we have shown that the SU(3)-symmetric PVV form is already ruled out by the present experimental upper limit, and we have then calculated the process with SU(3)-symmetry-broken vertices and found that with the Hamiltonian of Eq. (2) the process is predicted to occur at a rate quite close to the present experimental limit, namely

$$2.4\times10^{-4}<\Gamma_{K_2^0\to\pi^+\pi^-\gamma}/\Gamma_{K_2^0\to\text{all}}<4\times10^{-4}.$$

From the consideration of this process, we have further limited the possible range for ϵ_2. In Sec. IV, we have shown that the main contribution to $K^+ \to \pi^+\gamma\gamma$ comes from the four-leg vertices typical to our model, and again our predicted value is close to present experimental possibilities. The range of ϵ_2 obtained in Sec. III limits our predicted value for $K^+ \to \pi^+\gamma\gamma$ to

$$0.6\times10^{-5}<\Gamma_{K^+\to\pi^+\gamma\gamma}/\Gamma_{K^+\to\text{all}}<2\times10^{-5}.$$

What we have shown here so far is that the considered scheme is consistent with the available experimental information. The actual measurement of $K_2^0 \to \pi^+\pi^-\gamma$ and $K^+ \to \pi^+\gamma\gamma$ is needed, in order to verify the validity of our scheme. As our predicted values are probably within the range of experiments in progress, one should be able to draw interesting conclusions in the near future. In connection with the measurement of $K^+ \to \pi^+\gamma\gamma$ we stress the importance of obtaining experimental information on the pion kinetic energy spectrum.

Before concluding, we remark on the vector contribution to $K_{e_4}^+$ decay, which is also calculable with our model and affected by the SU(3)-symmetry-breaking parameters. We have calculated the vector part of $K^+ \to e^+\nu\pi^+\pi^-$ and found that with the breaking parameters of (46) its value is only slightly diminished from the SU(3)-symmetric value.[40] The experimental situation is too uncertain to permit a reliable estimate for the vector part, and the existing limit[41] is consistent with SU(3)-symmetric and SU(3)-symmetry-broken evaluation.

APPENDIX

In this appendix we give a brief review of Brown, Munczek, and Singer's paper,[2] whose scheme and results have been used here.

The effective Lagrangian responsible for the PVV and PPV interaction they use is

$$\mathcal{L}=\mathcal{L}_V+\mathcal{L}_P+\mathcal{L}_{PVV}, \tag{A1}$$

$$\mathcal{L}_P=\tfrac{1}{2}D_\mu P^a D_\mu P^a-\tfrac{1}{2}\mu_{ab}{}^2 P^a P^b. \tag{A2}$$

D_μ is the covariant derivative defined by

$$D_\mu F^a=\partial_\mu F^a-gf^{abc}V_\mu^b F^c. \tag{A3}$$

$\mathcal{L}_V$ is a Yang-Mills-type Lagrangian for the nine vector fields, including symmetry-breaking factors causing the mass differences between the vector mesons and current mixing.

$\mathcal{L}_{PVV}$ takes the most general form of octet-broken interaction

$$\mathcal{L}_{PVV} = \tfrac{1}{4}\epsilon^{\alpha\beta\mu\nu}(hD^{abc}V^a_{\alpha\beta}V^b_{\mu\nu}P^c + \lambda D^{ab}V^a_{\alpha\beta}V^0_{\mu\nu}P^b), \tag{A4}$$

where

$$V^a_{\mu\nu} = \partial_\mu V^a_\nu - \partial_\nu V^a_\mu - gf^{abc}V^b_\mu V^c_\nu, \tag{A5}$$

$$D^{abc} = d^{abc} + \sqrt{3}\,\epsilon_1 d^{ab0}d^{80c} + \tfrac{1}{2}\sqrt{3}\,\epsilon_2(d^{acd}d^{8db} + d^{bcd}d^{8da}) + (\epsilon_3/\sqrt{3})\delta^{ab}\delta^{c8}, \tag{A6}$$

$$D^{ab} = \delta^{ab} + \sqrt{3}\,\epsilon_4 d^{ab8}. \tag{A7}$$

$\mathcal{L}_V$ was diagonalized in terms of the physical particles, and the effective electromagnetic interaction is added in the vector-dominance formalism as follows:

$$\mathcal{L}_{\rm em} = \frac{em^2}{g}\left(\frac{1}{\sqrt{K_\rho}}\rho^0_\mu + \frac{\sin\theta}{\sqrt{3K_\omega}}\omega_\mu - \frac{\cos\theta}{\sqrt{3K_\phi}}\phi_\mu\right). \tag{A8}$$

The Lagrangians (A2), (A4), and (A8) are used to calculate various strong and electromagnetic decays. The SU(3)-symmetry-breaking corrections modify the amplitudes for the various decays by factors containing the masses of the vector mesons (the mass factors $K_i = m^2/m_i^2$ with $m = 847$ MeV), the vector-meson mixing angle ($\theta = 27.5°$), and the parameters ϵ_i.

A large class of electromagnetic and strong decays being considered, a consistent picture can be arrived at,[2,3] with the following values of the parameters:

$$\lambda = 2h(1+\epsilon_1)(\cot\theta)/\sqrt{3}\,(1+\epsilon_4),$$
$$\frac{g^2}{4\pi} = 3.20, \tag{A9}$$
$$\frac{m_\pi{}^2h^2}{4\pi}(1+\epsilon_1)^2 = 0.1,$$

and two admissible solutions for the following ϵ_i's:

$$\epsilon_1 = 0.85, \quad \epsilon_2 + \epsilon_3 = 2.16 \ \text{[solution (A)]}, \tag{A10}$$
$$\epsilon_1 = 1.18, \quad \epsilon_2 + \epsilon_3 = -2.54 \ \text{[solution (B)]}, \tag{A11}$$
$$\epsilon_4 = -0.32 \text{ or } 0.65 \ \text{for solution (A)}, \tag{A12}$$
$$\epsilon_4 = 1.53 \text{ or } -3.12 \ \text{for solution (B)}. \tag{A13}$$

---

*A preliminary account of this paper was presented at the APS Meeting, Rochester, N. Y., 1971.

†Based in part on a thesis by M. Moshe submitted to the Senate of the Technion, Israel Institute of Technology, in partial fulfillment of the requirements for the degree of Master of Science.

‡Present address: Department of Physics and Astronomy, Tel-Aviv University, Ramat-Aviv, Tel-Aviv, Israel.

[1]The decay $K_2^0 \to \gamma\gamma$ was discussed in detail in a previous publication [M. Moshe and P. Singer, Phys. Rev. Letters 27, 1685 (1971)] to which we refer the reader for details. Here we shall mention only the conclusions which are relevant for the whole class of decays analyzed.

[2]L. M. Brown, H. Munczek, and P. Singer, Phys. Rev. Letters 21, 707 (1968). For a review of this approach with references to recent experimental evidence on large SU(3)-symmetry-breaking effects in photoproduction and mesonic decays, see Ref. 3.

[3]P. Singer, in Proceedings of International Conference on Meson Resonances and Related Electromagnetic Phenomena, Bologna, 1971 (unpublished).

[4]L. M. Brown, H. Munczek, and P. Singer, Phys. Rev. 180, 1474 (1969).

[5]F. A. Constanzi, Phys. Rev. 182, 1571 (1969).

[6]One of the main predictions of Ref. 2 is a decrease from the SU(3) value by one order of magnitude of the $K^{*0}K^0\gamma$ vertex. Indirect evidence from K^0 photoproduction (Ref. 7) in $\gamma + p \to K^0 + \Sigma^+$ (supposedly proceeding through K^* exchange) seems to confirm this prediction. Other effects related to SU(3) symmetry breaking in processes involving K mesons are discussed in Refs. 1, 4, and 5.

[7]M. G. Albrow *et al.*, Phys. Letters 29B, 54 (1969); Nucl. Phys. B23, 509 (1970).

[8]J. J. Sakurai, Phys. Rev. 156, 1508 (1967).

[9]Y. Hara and Y. Nambu, Phys. Rev. Letters 16, 875 (1966).

[10]R. Rockmore, Phys. Rev. 182, 1512 (1969).

[11]R. Rockmore, Phys. Rev. 185, 1847 (1969).

[12]B. W. Lee and A. R. Swift, Phys. Rev. 136, B229 (1964); H. Sugawara, Phys. Rev. Letters 15, 870 (1965); 15, 997 (E) (1965); M. Suzuki, *ibid.* 15, 986 (1965).

[13]See also I. Kimel, Nucl. Phys. B23, 574 (1970).

[14]C. H. Albright and R. Oakes, Phys. Rev. D 2, 1883 (1970); 3, 1270 (1971).

[15]N. J. Carron and R. L. Schult, Phys. Rev. D 1, 3171 (1970). See here for previous articles on this process.

[16]M. G. Smoes, Nucl. Phys. B20, 237 (1970).

[17]R. J. Macek, A. K. Mann, W. K. McFarlane, and J. B. Roberts, Phys. Rev. D 1, 1249 (1970).

[18]From an analysis of electromagnetic mass differences of pseudoscalar mesons, a value for ϵ_2 was deduced (Ref. 4) which would explain the $K^+ - K^0$ mass difference in conjunction with a tadpole contribution. The value predicts a $K^{*+} \to K^+\gamma$ width some 30 times larger than the SU(3) value, while the values we arrive at in Eqs. (14a) and (14B) allow for a maximum increase of $K^{*+} \to K^+\gamma$ by 11. Due to uncertainties in the two figures compared, this cannot be considered yet as an inconsistency.

[19]C. S. Lai and B. L. Young, Nuovo Cimento 57A, 83 (1967).

[20]R. C. Thatcher *et al.*, Phys. Rev. 174, 1674 (1968).

[21]R. Rockmore, Phys. Rev. D 1, 226 (1970).

[22]S. V. Pepper and Y. Ueda, Nuovo Cimento 33, 1614

(1964); S. Oneda, Y. S. Kim, and D. Korff, Phys. Rev. 136, B1064 (1964).

[23]M. A. Preston, *Physics of the Nucleus* (Addison-Wesley, Reading, Mass., 1965); see also H. Chew, Nuovo Cimento 26, 1109 (1962).

[24]Rockmore (Ref. 10) exploits partial conservation of axial-vector current in order to express the combined contributions of the pseudoscalar and axial-vector poles in terms of the pseudoscalar-pole contribution only. To give an example, for the first and second diagrams in Fig. 2, the contribution of the pseudoscalar poles gives

$$\langle \pi^+\pi^-\gamma|H_W(0)|K_2^0\rangle \xrightarrow[\text{ps poles } (\alpha)]{} C_6 C_\alpha m_{K_2^0}{}^2 \langle \pi^+\pi^-\gamma|\phi^\alpha|0\rangle ,$$

while the combined contribution of pseudoscalar and axial-vector poles using Rockmore's procedure gives

$$\langle \pi^+\pi^-\gamma|H_W(0)|K_2^0\rangle \xrightarrow[\text{ps + axial-vector poles}]{} C_6 C_\alpha m_\alpha{}^2 \langle \pi^+\pi^-\gamma|\phi^\alpha|0\rangle$$

with $\alpha = 3$ and 8.

[25]S. L. Glashow and S. Weinberg, Phys. Rev. Letters 20, 224 (1968); Riazzudin and A. K. Sarker, *ibid.* 20, 1455 (1968). Small reasonable changes in the values of (C_K/C_π), (C_η/C_π) do not practically affect our calculation.

[26]A. H. Rosenfeld *et al.*, Rev. Mod. Phys. 43, S1 (1971).

[27]J. H. Klems, R. H. Hildebrand, and R. Stiening, Phys. Rev. Letters 25, 473 (1970); Phys. Rev. D 4, 66 (1971).

[28]In this experiment one searched for pions with kinetic energies in the range 117–127 MeV. The upper limit for the decay was then obtained by assuming a constant matrix element for it.

[29]I. R. Lapidus, Nuovo Cimento 46A, 608 (1966).

[30]Y. Hara and Y. Nambu, Phys. Rev. Letters 16, 875 (1966); S. Okubo, R. E. Marshak, and V. S. Mathur, *ibid.* 19, 407 (1967).

[31]Y. Fujii, Phys. Rev. Letters 17, 613 (1966).

[32]G. Fäldt, B. Peterson, and H. Pilkuhn, Nucl. Phys. B3, 234 (1967).

[33]G. W. Intemann, Phys. Rev. D 2, 2630 (1970).

[34]Full details of these calculations are given in M. Moshe, M.Sc. thesis, Technion-Israel Institute of Technology, 1971 (unpublished).

[35]J. Ballam *et al.*, Phys. Rev. D 1, 94 (1970).

[36]C. Maiani and G. Preparata, Nuovo Cimento 48A, 550 (1967).

[37]A. H. Zimmerman and C. A. Savoy, Nuovo Cimento 57A, 201 (1968).

[38]D. Greenberg, Phys. Rev. 178, 2190 (1969). Our treatment differs in details from Greenberg's, as we include the axial-vector intermediate state with Rockmore's procedure (Ref. 10).

[39]See also R. F. Sarraga and H. J. Munczek, Phys. Rev. D 4, 2884 (1971).

[40]C. E. Wood, Phys. Rev. 181, 1890 (1969); Phys. Rev. D 1, 3203(E) (1970).

[41]R. P. Ely *et al.*, Phys. Rev. 180, 1319 (1969).